Symmetric Conformal Mapping for Surface Matching and Registration

Wei Zeng * † Jing Hua * Xianfeng David Gu †
* *Computer Science Department, Wayne State University, Detroit, Michigan 48202, USA*
† *Computer Science Department, Stony Brook University, Stony Brook, New York 11794, USA*

Abstract

Recently, various conformal geometric methods have been presented for non-rigid surface matching and registration. This work proposes to improve the robustness of conformal geometric methods to the boundaries by incorporating the symmetric information of the input surface.

We presented two symmetric conformal mapping methods, which are based on solving Riemann-Cauchy equation and curvature flow respectively. Experimental results on geometric data acquired from real life demonstrate that the symmetric conformal mapping is insensitive to the boundary occlusions. The method outperforms all the others in terms of robustness. The method has the potential to be generalized to high genus surfaces using hyperbolic curvature flow.

1. Introduction

In recent decades, there has been a lot of research into surface representations for 3D surface analysis, which is a fundamental issue for many applications in computer graphics, computer vision and geometric modeling, such as 3D shape registration, partial scan alignment, 3D object reconstruction, 3D object recognition, and classification [1], [2], [3], [4].

In particular, as 3D scanning technologies improve, large databases of 3D scans require automated methods for matching and registration. However, matching surfaces undergoing non-rigid deformation is still a challenging problem, especially when data is noisy and with complicated topology. Different approaches have been introduced in the literature [4], [5], [6], [7], [8], [9], [10], [11], [12], [13], [14], [15], [16], [17]. However, many surface representations that use local geometric invariants can not guarantee a global convergence and might suffer from local minima in the presence of non-rigid deformations.

Recently, many global parameterizations methods have been developed based on conformal geometric maps [18], [19], [20], [21], [22], [23]. Although the previous methods have met with a great deal of success in both computer vision and graphics, there is a major shortcoming in conformal maps when applied to matching of real discrete data such as the output of 3D scanners: *inconsistent boundaries*. In real applications in graphics and CAD, many categories of surfaces of interests are symmetric, such as human faces, human bodies, most furniture, buildings, automobiles etc. To address the above critical issue, we propose to incorporate the symmetry of the input surface to the conformal mapping, such that the conformal mapping preserves the intrinsic symmetry of the surface and is more robust to the inconsistency of the boundaries. The conformal mapping preserves the symmetry in the following ways: first the image of the mapping is still symmetric; second, the area distortion factor on the image is symmetric as well. Figure 9 shows the symmetric conformal mappings, which are much more robust to the boundary occlusions and inconsistency.

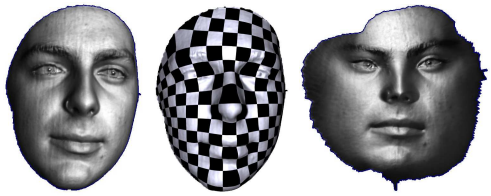

(a) calm face

(b) smile face

Figure 1. Symmetric Conformal Mapping for human faces, Sub1.A and Sub1.B, with different expressions. The property of symmetry preserving is illustrated from the flat image and the check-board texture mapping image, where the conformality and the area distortion are visualized.

1.1. Conformal Geometric Methods

There are four categories of conformal geometric methods for the application of surface matching and registration, including *Harmonic Maps* [18], [19], [20], *Riemann-Cauchy Equation* (such as least square conformal maps (LSCMs)

• *Corresponding author: W. Zeng*
E-mail: zeng@wayne.edu, zengwei@cs.sunysb.edu

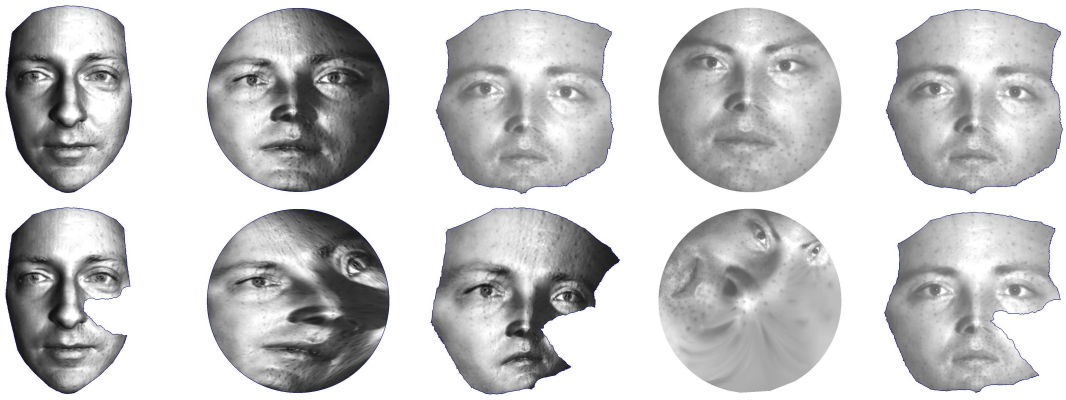

(a) original / occluded face | (b) harmonic map | (c) least square conformal map | (d) holomorphic 1-form map | (e) symmetric conformal map

Figure 2. Comparison among different conformal mapping methods for faces Sub2.A and Sub2.B. The occluded face shares the same symmetry plan with the original face. Symmetric conformal map is the most robust to boundary occlusion.

introduced in [21]) [23], [24], *Holomorphic Differentials* [25], and *Ricci Flow* [26], [27]. Recently, discrete surface Yamabe flow has been introduced by Luo in [28], which has been reintroduced in [29]. Hyperbolic Yamabe flow is presented in [30]. A similar method is applied for conformal parameterization in [31].

In general, harmonic maps, LSCMs are linear methods, but can only handle surfaces with simple topologies, such as topological disks. Holomorphic differentials can handle multiply connected domains and high genus surfaces, but it introduces singularities. Ricci flow method is very general and has no topological limitations, but it is a nonlinear optimization. All of them are very sensitive to the boundaries. As shown in Figure 2, inconsistent boundary conditions produce drastically different conformal mappings and lead to the failure for partial matching and registration. Figure 3 gives an example to show that the conformal mapping has the property of intrinsic symmetry preserving.

1.2. Contributions

We make the following contributions in our paper:

- A conformal mapping method based on solving Riemann-Cauchy equation is introduced, which preserves the symmetry of the input surface.
- A conformal mapping method based on discrete curvature flow (Yamabe Flow) is introduced, which preserves the symmetry of the input surface.
- A robust method for non-rigid surface matching and registration based on symmetric conformal mapping is introduced, which is very robust to boundary occlusion and clutter.

Although the work focuses on topological disks, it can be generalized to surfaces with more complicated topologies, such as multiply connected domains or high genus surfaces, as long as the surface has intrinsic symmetry. The Riemann-Cauchy equation method can only handle topological disks, while the curvature flow method can be generalized to handle arbitrary topologies. Similarly, the symmetric constraints can also be incorporated in the other two methods.

2. Mathematical Background

All surfaces embedded in $\mathbb{R}^3$ have the induced Euclidean metric $\mathbf{g}$. A *conformal structure* is an atlas, such that on each local chart, the metric can be represented as $\mathbf{g} = e^{2u}(dx^2 + dy^2)$. we can use complex parameter to represent it $z = x + iy$, which is called *isothermal coordinates*. Suppose two charts have overlapping region on the surface, then the chart transition function is an analytic function. A surface with a conformal structure is a *Riemann surface*, therefore, all surfaces in $\mathbb{R}^3$ are Riemann surfaces.

A complex valued function $f : \mathbb{C} \to \mathbb{C}$ is *holomorphic*, if it satisfies the following Riemann-Cauchy equation, $f : z \to w$, where $z = x + iy$ and $w = u + iv$,

$$\frac{\partial u}{\partial x} = \frac{\partial v}{\partial y}, \quad \frac{\partial u}{\partial y} = -\frac{\partial v}{\partial x}. \tag{1}$$

A mapping between two Riemann surfaces $f : S_1 \to S_2$ between two surfaces is *conformal*, if it satisfies the following condition: Arbitrarily choosing a local isothermal coordinates of S_1, (U_α, ϕ_α), a local isothermal coordinates of S_2, (V_β, ϕ_β), then the local presentation of f is $\phi_\beta \circ f \circ \phi_\alpha^{-1}$ is holomorphic. In this work, S_1 is a genus zero surface with a single boundary, S_2 is a planar domain.

There are mainly four categories to compute conformal mappings.

2.1. Harmonic Maps

Let $f : S \to D$ be a mapping between two surfaces, then the *harmonic energy* of f is defined as $E(f) = \int_S |\nabla f|^2 dA$,

where ∇f is the gradient of f, dA is the area element on S. The harmonic map is the critical point of the harmonic energy, which satisfies the Laplace equation $\Delta f = 0$.

The harmonic map can be achieved using the heat flow method $\frac{df}{dt} = -\Delta f$, where Δ is the Laplace-Beltrami operator on S. In general, if the target domain is convex, the boundary mapping $f : \partial S \to \partial D$ is a homeomorphism, then the harmonic map is a diffeomorphism. Especially, if D is a genus zero closed surface, then the harmonic map is also a conformal map. Figure 2(b) is computed using harmonic maps as described in [19].

2.2. Solving Riemann-Cauchy Equation

Conformal maps satisfy the Riemann-Cauchy equation (1). Therefore by solving Riemann-Cauchy equation with boundary conditions, a conformal map can be obtained. in practice, one can solve the equation by minimizing the following energy,

$$E(f) = \int_S (\frac{\partial u}{\partial x} - \frac{\partial v}{\partial y})^2 + (\frac{\partial u}{\partial y} + \frac{\partial v}{\partial x})^2 dxdy. \qquad (2)$$

Figure 2(c) is computed by minimizing the above energy using the method described in [21].

2.3. Holomorphic 1-Form

Let ω be a complex-valued differential form on the Riemann surface S, such that on each local chart (U_α, ϕ_α) with isothermal coordinates z_α, ω has local representation $\omega = g_\alpha(z_\alpha)dz_\alpha$, where g_α is holomorhpic, then ω is called a *holomorphic 1-form*. On another local chart (U_β, ϕ_β) with isothermal coordinates z_β, ω has local representation $\omega = g_\beta(z_\beta)dz_\beta$ where $g_\alpha \frac{dz_\alpha}{dz_\beta} = g_\beta$, where $\frac{dz_\alpha}{dz_\beta}$ is a holomorphic function. All the holomorphic 1-forms form a group, which is isomorphic to the first cohomology group of the surface.

The holomorphic 1-form group basis can be computed as follows: first we compute the homology group basis of the surface, the the dual cohomology group basis, then use Hodge theory to get the unique harmonic 1-form for each cohomologous class; finally, use Hodge star to compute the conjugate harmonic 1-forms. Each pair of harmonic 1-form and its conjugate form a holomorphic 1-form. This method has been introduced in [32]. Figure 2(d) is computed using holomorphic 1-forms.

2.4. Ricci Curvature Flow

Let S be a surface embedded in $\mathbb{R}^3$. S has a Riemannian metric induced from the Euclidean metric of $\mathbb{R}^3$, denoted by $\mathbf{g}$. Suppose $u : S \to \mathbb{R}$ is a scalar function defined on S. It can be verified that $\bar{\mathbf{g}} = e^{2u}\mathbf{g}$ is also a Riemannian metric on S. We say $\bar{\mathbf{g}}$ is *conformal* to $\mathbf{g}$, e^{2u} is called the *conformal factor*.

When the Riemannian metric is conformally deformed, Gaussian curvatures will also be changed accordingly to the *Yamabe equation*, $\bar{K} = e^{-2u}(-\Delta_{\mathbf{g}} u + K)$, where $\Delta_{\mathbf{g}}$ is the Laplace-Beltrami operator under the original metric $\mathbf{g}$. Yamabe equation can be solved using *Ricci flow* method by a prescribed curvature $\bar{K}$,

$$\frac{dg_{ij}(t)}{dt} = 2(\bar{K} - K(t))g_{ij}(t).$$

where t is the time parameter. If the target curvature is zero on every interior point, then the surface can be flattened onto a planar domain with the resulting metric.

Surface Ricci flow has been generalized to the discrete setting by Luo and Chow in [33]. In surface case, Ricci flow is equivalent to Yamabe flow. Discrete Yamabe flow was first introduced by Luo in [28]. Figure 10 is computed using curvature flow method [30].

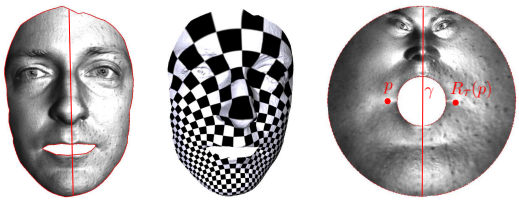

Figure 3. Conformal mapping preserving symmetry. γ is the intersection curve between the surface and the symmetric plane. p and $R_\tau(p)$ are symmetric points. The symmetry is preserved on the image of the conformal mapping ϕ.

3. Symmetric Conformal Mapping Method

All the existing conformal mapping methods are sensitive to boundary conditions. Surface registration algorithms based on conformal geometric methods are susceptible to occluded boundaries, clutters and inconsistent boundaries. We propose to improve the robustness of conformal mapping methods by utilizing the symmetry of the input surface.

Suppose the input surface S has some symmetries. For example (see Figure 3), suppose τ is a plane in $\mathbb{R}^3$, R_τ is the reflection about τ. If S is symmetric about τ, then $R_\tau(S) = S$. Let γ be the intersection curve of the surface and the symmetric plane, $\gamma = S \cap \tau$, $\phi : S \to \mathbb{C}$ is a conformal mapping of the surface to the complex plane. We say the conformal mapping preserves symmetry, if

$$\phi(R_\tau(p)) = -\overline{\phi(p)},$$

where $\overline{\phi(p)}$ means the conjugate of $\phi(p)$. Namely, ϕ maps γ to the imaginary axis, the images of the symmetric points p and $R_\tau(p)$ are symmetric about the imaginary axis. This can be accomplished by adding symmetric constraints (complex position, or conformal factor) during the optimization process.

In practice, surfaces are approximated by triangle meshes, conformal mappings are approximated by piecewise linear maps.

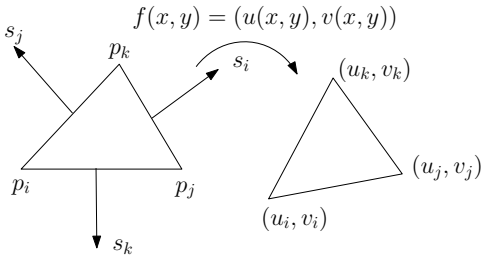

Figure 4. Discrete approximation of Riemann-Cauchy equation.

3.1. Riemann-Cauchy Equation Method

This method is a direct generalization of LSCM in [21] by adding symmetric constraints. Let $[p_i, p_j, p_k]$ be a face on the mesh (see Figure 4). The images of them under the linear map $f : [p_i, p_j, p_k] \to \mathbb{R}^2$ are $(u_i, v_i), (u_j, v_j), (u_k, v_k)$. Let $\mathbf{s}_i = \mathbf{n} \times (p_k - p_j), \mathbf{s}_j = \mathbf{n} \times (p_i - p_k), \mathbf{s}_k = \mathbf{n} \times (p_j - p_i)$, $\mathbf{n}$ is the normal vector of the face, then

$$\begin{aligned} -\nabla u &= u_i \mathbf{s}_i + u_j \mathbf{s}_j + u_k \mathbf{s}_k, \\ -\nabla v &= v_i \mathbf{s}_i + v_j \mathbf{s}_j + v_k \mathbf{s}_k, \end{aligned}$$

Riemann-Cauchy energy on face $[p_i, p_j, p_k]$ can be approximated by $E([p_i, p_j, p_k]) = |\nabla v - \mathbf{n} \times \nabla u|^2$. The energy (2) can be approximated as

$$\sum_{[p_i, p_j, p_k] \in M} E([p_i, p_j, p_k]) A([p_i, p_j, p_k]),$$

where $A([p_i, p_j, p_k])$ represents the area of the face.

The symmetric constraints can be inserted naturally during the optimization of the above energy. Suppose p_i, p_j are symmetric vertices of the mesh, $R_\tau(p_i) = p_j$, then we add constraint $u_i = -u_j,\ v_i = v_j$.

3.2. Yamabe Flow Method

Symmetry constraints can also be added to the curvature flow method naturally. Here we use Yamabe flow method introduced in [28]. On a triangle mesh, the *discrete metric* is the edge length function $\ell : E \to \mathbb{R}^+$ satisfying triangle inequality. The *vertex discrete curvature* is defined as angle deficiency,

$$K_i = \begin{cases} 2\pi - \sum_{[p_i, p_j, p_k] \in F} \theta_i^{jk} & p_i \notin \partial M \\ \pi - \sum_{[p_i, p_j, p_k] \in F} \theta_i^{jk} & p_i \in \partial M \end{cases}$$

where θ_i^{jk} is the corner angle at p_i in the face $[p_i, p_j, p_k]$, ∂M is the boundary of M. Let $\mathbf{u} : V \to \mathbb{R}$ be the discrete conformal factor. The edge length of $[p_i, p_j]$ is defined as $\ell_{ij} := \exp(u_i) \exp(u_j) \ell_{ij}^0$, where ℓ_{ij}^0 is the original edge length in $\mathbb{R}^3$. The discrete Yamabe flow is defined as

$$\frac{du_i}{dt} = \bar{K}_i - K_i,$$

with the constraint $\sum_i u_i = 0$. The discrete Yamabe flow converges, and the final discrete metric induces the prescribed curvature; a detailed proof can be found in [28].

During the Yamabe flow, we can enforce the symmetry in the following way. Assume p_i and p_j are two symmetric interior vertices, $R_\tau(p_i) = p_j$, $p_i, p_j \notin \partial M$, therefore their target curvatures are the same $\bar{K}_i = \bar{K}_j$, then during the Yamabe flow, we always ensure $u_i = u_j$.

4. Computational Algorithm

The computational algorithm for symmetric conformal mapping is straight forward. It includes the following steps.

4.1. Finding Symmetric Plane

Assume the input surface has a reflective symmetric plane τ, this step aims at find the plane. Although there are rich literature on finding symmetry of images, we focus on finding the symmetry of a 3D surface. The generalized Hough transformation has been introduced in [34] for finding the symmetry plane of 3D point clouds. We adapt the method to locate the symmetry plane for our dense point clouds of human face surfaces.

4.2. Finding Feature Points

The scanned data sets have both texture information and geometric information. In current work, we only utilize the texture information for locating feature points. We apply conventional SIFT method [35] on the texture image to find major feature points, such as eye corners, mouth corners etc. The symmetry of feature points can be computed by the method in [36]. Then we project back the feature points from the texture image to the 3D surfaces.

4.3. Cross Registration

$$\begin{array}{ccc} S_1 & \xrightarrow{f} & S_2 \\ {\scriptstyle \phi_1}\downarrow & & \downarrow{\scriptstyle \phi_2} \\ D_1 & \xrightarrow[g]{} & D_2 \end{array}$$

Given two 3D face surfaces S_1 and S_2 of the same person with different expressions and different boundaries, we want to register them using symmetric conformal mapping. First, we compute symmetric conformal maps $\phi_1 : S_1 \to \mathbb{D}_1$, $\phi_2 : S_2 \to \mathbb{D}_2$, using the symmetric information obtained in the first step. Then we compute a constrained harmonic map $g : \mathbb{D}_1 \to \mathbb{D}_2$, such that g align the major corresponding features and also preserves symmetry. The correspondence between the major features are specified by the user. The matching and registration accuracy is directly influenced by the detected feature constraints. The map $g = (g_1, g_2)$ minimizes the harmonic energy

$$E(g) = \int_{\mathbb{D}_1} (\frac{\partial g_1}{\partial x} + \frac{\partial g_1}{\partial y})^2 + (\frac{\partial g_2}{\partial x} + \frac{\partial g_2}{\partial y})^2 dxdy,$$

such that $g_1(-x, y) = -g_1(x, y)$, $g_2(-x, y) = g_2(x, y)$. Then the registration is given by

$$f = \phi_2^{-1} \circ g \circ \phi_1 : S_1 \to S_2.$$

5. Experimental Results

We implemented our algorithm using generic C++ on Windows XP and used conjugate gradient optimization for acceleration. The human face data sets are acquired using high speed 3D scanner based on phase-shifting method in [19]. The scanning speed is 30 frames per second, the resolution for each frame is 640×480. The experiments are conducted on a HP xw4600 Workstation with Intel Core 2Duo CPU 2.33GHz, 3.98 GB of RAM. The running time is reported Table 1.

Table 1. Computational time of symmetric conformal mappings.

Name	David1	David2	Luke1	Anna1	Anna2
#Face	148,305	147,038	50,000	156,401	147,430
#Vertex	74,699	74,063	25,246	78,773	74,281
Time (s)	8	17	16	28	14

Figure 5. Symmetric LSCM for faces Sub3.A and Sub3.B with inconsistent boundaries.

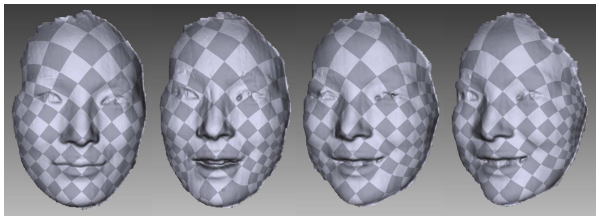

frame 030 frame 110 frame 164 frame 210

Figure 6. Registration for a sequence of Sub3's face surfaces with different expressions and postures.

The symmetric conformal mapping for various human face surfaces are illustrated in Figures 1, 2, and 5. The (partial) registration results for face surfaces with different expressions and postures are illustrated in Figure 6. Although the boundaries are significantly different, and the registrations are performed on the relatively small overlapping regions, the texture pattern on the overlapping regions among the four frames are very consistent. This demonstrates the robustness of our method. Figures 7, 8 and 9 show our method tested on the other facial expression sequences with different non-rigid deformations, where the boundaries are almost fixed and the registrations are also visualized by the check-board texture mapping. The matching error is measured by computing the relative Hausdorff average distance (RHAD) under iterative closest point (ICP), harmonic map method (HM) [19], and our symmetric conformal map method (SCM). We matched the first frame to others within each class and got the average matching error as follows: Sub1(0.054, 0.015, 0.008), Sub2(0.221, 0.035, 0.020), Sub3(0.090, 0.020, 0.013) and Sub4(0.028, 0.009, 0.006) for (ICP, HM, SCM). For all the tested experiments, our method outperforms both the ICP and HM methods.

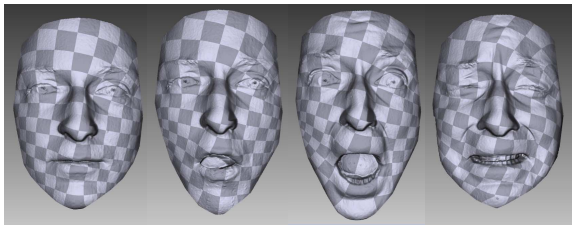

frame 001 frame 100 frame 200 frame 399

Figure 7. Registration for a sequence of Sub2's face surfaces with significantly different expressions.

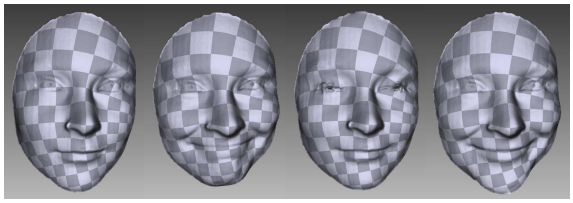

frame 001 frame 100 frame 174 frame 360

Figure 8. Registration for a sequence of Sub4's face surfaces with eye and mouth motions.

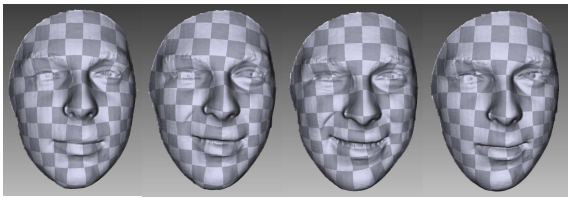

frame 001 frame 140 frame 230 frame 360

Figure 9. Registration for a sequence of Sub1's face surfaces with asymmetrical expression deformations.

Figure 10(a) demonstrates the symmetric Yamabe flow method as described in previous section. The target curvatures are set to preserve the symmetry. During the flow, the conformal factors u are constrained to be symmetric. The final conformal mapping image is also symmetric. This example shows the flexibility of our method, that can handle surfaces with complicated topologies.

(a) multiply connected domain (b) high genus surface

Figure 10. Symmetric Conformal Mapping using Yamabe flow. (a) Euclidean Yamabe flow for multiply connected domain, (b) Hyperbolic Yamabe flow for high genus surface.

6. Conclusion and Future Works

Conventional conformal mapping methods are susceptible to inconsistent boundaries. This work proposes to improve the robustness of conformal geometric methods by incorporating the symmetric information into the mapping process. Novel conformal mapping algorithms based on solving Riemann-Cauchy equation and curvature flow are developed, which preserve the symmetry of the input surface. Experimental results demonstrate the symmetric conformal mapping is insensitive to the boundary occlusions.

Although current work focuses on genus zero surfaces, it can be directly generalized to high genus surfaces as well. Figure 10(b) demonstrates such an example, a genus two surface is conformally mapped to the hyperbolic space periodically using hyperbolic Yamabe flow method. In the future, we will continue the exploration for high genus surfaces. Furthermore, we will investigate to generalize the method for surfaces with symmetries other than mirror reflection and incorporate more geometric structural characteristics to conformal mappings to improve the robustness and accuracy.

References

[1] R. Campbell and P. Flynn. *A survey of free-form object representation and recognition techniques*. Computer Vision and Image Understanding, 81:166-210, 2001.

[2] J. Wyngaerd, L. Gool, R. Koch, and M. Proesmans. *Invariant-based registration of surface patches*. In ICCV, pages 301-306, 1999.

[3] D. Huber, A. Kapuria, R. Donamukkala, and M. Hebert. *Parts-based 3d object classification*. In CVPR, pages II: 82-89, June 2004.

[4] S. Ruiz-Correa, L. Shapiro, and M. Meila. *A new paradigm for recognizing 3d object shapes from range data*. In ICCV, pages 1126-1133, 2003.

[5] P. Xiao, N. Barnes, T. Caetano, and P. Lieby. *An mrf and gaussian curvature based shape representation for shape matching*. In CVPR, 2007.

[6] Y. Sun and M. Abidi. *Surface matching by 3d point's fingerprint*. In ICCV, pages II: 263-269, 2001.

[7] T. Funkhouser, P. Min, M. Kazhdan, J. Chen, A. Halderman, D. Dobkin, and D. Jacobs. *A search engine for 3d models*. In ACM TOG, pages 83-105, 2003.

[8] R. Osada, T. Funkhouser, B. Chazelle, and D. Dobkin. *Shape distributions*. In ACM TOG, volume 21, pages 807-832, 2002.

[9] A. M. Bronstein, M. M. Bronstein, and R. Kimmel. *Rock, paper, and scissors: extrinsic vs. intrinsic similarity of nonrigid shapes*. In ICCV, 2007.

[10] J. Starck and A. Hilton. *Correspondence labelling for widetimeframe free-form surface matching*. In ICCV, 2007.

[11] W.-Y. Lin, K.-C. Wong, N. Boston, and H.-H. Yu. *Fusion of summation invariants in 3d human face recognition*. In CVPR, 2006.

[12] P. Dalal, B. C. Munsell, S. Wang, J. Tang, K. Oliver, H. Ninomiya, X. Zhou, and H. Fujita. *A fast 3d correspondence method for statistical shape modeling*. In CVPR, 2007.

[13] D. Terzopoulos, A. Witkin, and M. Kass. *Constraints on deformable models: Recovering 3d shape and nonrigid motion*. Artificial Intelligence, 35:91-123, 1988.

[14] X. Huang, N. Paragios, and D. Metaxas. Establishing local correspondences towards compact representations of anatomical structures. In MICCAI03, pages 926-934, 2003.

[15] R. Malladi, J. A. Sethian, and B. C. Vemuri. A fast level set based algorithm for topology-independent shape modeling. JMIV, 6(2/3):269-290, 1996.

[16] B. Brown and S. Rusinkiewicz. *Global Non-Rigid Alignment of 3-D Scans*. ACM Transactions on Graphics, August 2007.

[17] H. Li, R. Sumner, and M. Pauly. *Global Correspondence Optimization for Non-Rigid Registration of Depth Scans*. Compu. Graph. Forum, 2008.

[18] D. Zhang and M. Hebert. Harmonic maps and their applications in surface matching. In CVPR, pages II: 524-530, 1999.

[19] Y. Wang, M. Gupta, S. Zhang, S. Wang, X. Gu, D. Samaras, and P. Huang. *High resolution tracking of non-rigid 3d motion of densely sampled data using harmonic maps*. In ICCV, pages I: 388-395, 2005.

[20] X. Gu, Y. Wang, T. F. Chan, P. M. Thompson, and S. Yaun. *Genus zero surface conformal mapping and its application to brain surface mapping*. TMI, 23(7), 2004.

[21] B. Levy, S. Petitjean, N. Ray, and J. Maillot. *Least squares conformal maps for automatic texture atlas generation*. In SIGGRAPH02, pages 362-371, 2002.

[22] E. Sharon and D. Mumford. *2d-shape analysis using conformal mapping*. In CVPR, pages II: 350-357, 2004.

[23] S. Wang, Y. Wang, M. Jin, X. D. Gu, and D. Samaras. *Conformal geometry and its applications on 3d shape matching, recognition, and stitching*. PAMI, 29(7):1209-1220, 2007.

[24] S. Wang, X. Gu, and H. Qin. *Automatic non-rigid registration of 3d dynamic data for facial expression synthesis and transfer*. In CVPR, 2008.

[25] W. Zeng, Y. Zeng, Y. Wang, X. Gu and D. Samaras. *3D non-rigid surface matching and registration based on holomorphic differentials*. In ECCV, 2008.

[26] X. Gu, S. Wang, J. Kim, Y. Zeng, Y. Wang, H. Qin, and D. Samaras. *Ricci flow for 3d sahpe analysis*. In ICCV, 2007.

[27] W. Zeng, X. Yin, Y. Zeng, Y. Lai, X. Gu and D. Samaras. *3D face matching and registration based on hyperbolic Ricci flow*, In CVPR Workshop on 3D Face Processing, 2008.

[28] F. Luo. *Combinatorial yamabe flow on surfaces*. Commun. Contemp. Math., 6(5):765-780, 2004.

[29] B. Springborn, P. Schröder, U. Pinkall. *Conformal equivalence of triangle meshes*. ACM Trans. Graph.,27(3):1-11,2008.

[30] W. Zeng, M. Jin, F. Luo, and X. Gu. *Computing canonical homotopy class representative using hyperbolic structure*. In IEEE International Conference on Shape Modeling and Applications (SMI09), 2009.

[31] M. Ben-Chen, C. Gotsman, G. Bunin. *Conformal Flattening by Curvature Prescription and Metric Scaling*, Comp. Graph. Forum, 27(2):449-458,2008.

[32] X. Gu, S.-T. Yau, *Global conformal parameterization*, in SGP 2003.

[33] B. Chow and F. Luo, *Combinatorial ricci flows on surfaces*, Journal Differential Geometry, 63(1):97-129, 2003.

[34] N. J. Mitra, L. J. Guibas, and M. Pauly. *Partial and approximate symmetry detection for 3d geometry*. ACM Trans. Graph., 25(3):560-568, 2006.

[35] D. Lowe. *Object recognition from local scale-invariant features*. In ICCV, pages 1150-1157, 1999.

[36] M. Park, S. Lee, P.-C. Chen, S. Kashyap, A. A. Butt, and Y. Liu. *Performance evaluation of state-of-the-art discrete symmetry detection algorithms*. In CVPR, 2008.